An Efficient Approach to Automatic Power Factor Improvement

M. I. Uddin[1*], R. Barua[2]
[1,2]Department of Electrical and Electronic Engineering, [1,2]Chittagong University of Engineering and Technology, Chattogram, Bangladesh

[*]corresponding author's email: iftekher7eee@gmail.com

Abstract—*An automatic power factor improvement (APFI) system improves the power factor (PF) of a load by switching capacitor banks automatically. A low PF increases the supply current and losses, and the capacitance needed for correction depends on which loads are connected. This paper presents the simulation and experimental evaluation of the switching mechanism of an APFI system. Four loads yield 15 nonzero load combinations. A mathematical model determines the capacitance required to reach a target PF of 0.97 for each load combination. An Arduino microcontroller detects the connected load combination through sensing relays and switches the appropriate capacitor banks across the connected loads using mechanical relays. A liquid-crystal display (LCD) shows the connected loads, the target PF and the displayed load PF. The switching logic was checked in a Proteus simulation, and the relay-switching states were tested on a laboratory prototype with loads rated 60–250 W. The power values shown on the simulated LCD are programmed test values and not measurements. The calculated results indicate that approximately 79% of the reactive power can be compensated when all four loads are connected to the power system. The mechanical relays provide a simple switching mechanism.*

Keywords: *Energy efficiency, Inductive load, Microcontroller, Power Factor, Reactive power*

Article History
Received 10 May 2026
Received in revised form 23 June 2026
Accepted 13 July 2026
Published online October 2026

I. Introduction

Energy efficiency is an important consideration in electrical systems. Power factor (PF) is an electrical characteristic, defined by cosθ, which significantly influences energy usage in alternating current (AC) circuits. It quantifies the conversion of electrical power into real (active) power. Low PF is a concern for industrial users and utilities. For a given real-power demand and supply voltage, a lower PF requires a higher supply current. Improving PF reduces the supply current and conductor losses for a given real-power demand. In Fig. 1, the phase angle denoted by θ is the angle between the real power and apparent power and is classified as either leading or lagging. The ratio of real power P (in W) to apparent power S (in VA) is the PF, that is, PF = P/S.

In an inductive AC circuit, the current lags behind the voltage at lagging PF. The angle between the real power and reactive power is 90 degrees. Automatic power factor improvement (APFI) systems are used to monitor, evaluate, and optimize the PF in real time [1]. Installing APFI systems can reduce energy losses and operational expenses and improve overall system performance.

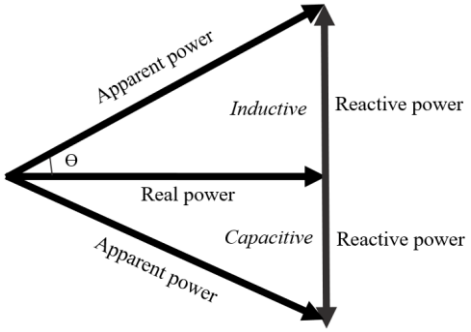


Fig. 1. Power triangle

These systems provide real-time monitoring and control functionalities and are appropriate for dynamic PF adjustment. A microcontroller is an integrated chip that includes a central processing unit (CPU), random access memory (RAM), and input-output devices (I/O) and can perform a given task. Numerous studies have examined the utilization of microcontrollers in PF improvement devices. Various studies investigate diverse algorithms and control strategies utilizing the microcontrollers for effective PF correction. Continuous energy monitoring

This is an Open Access article distributed under the terms of the Creative Commons Attribution-Noncommercial 3.0 Unported License, permitting copy and redistribution of the material and adaptation for commercial and uncommercial use.

through the internet of things (IoT) using Raspberry Pi has elevated the PF from 0.7 to 0.99 and augmented the security and control of power systems [2]. Real-time monitoring data, facilitated by sensors, are used to identify the deviations from standard operating conditions. Table I compares the proposed approach with previous studies in terms of load detection, switching strategy, PF before and after correction, power scale and implementation cost. In Table I, CT and PT denote current and potential transformers; ZCD, zero-crossing detector; DFT, discrete Fourier transform; RL, resistive–inductive; TRIAC, triode for alternating current; MOSFET, metal–oxide–semiconductor field-effect transistor; and ATP, Alternative Transients Program.

TABLE I
COMPARISON OF APFI SYSTEMS

Ref.	Authors / Year	Load Detection Method	Switching Strategy	PF Before and After Correction	Power Scale	Implementation Cost
[3]	R.A. Mahmoud et al. (2022)	Cross-coherence coefficient between voltage and current signals (DFT-based)	Relay	0.49 to 0.994	6.75 kW (9 HP) induction motor	Higher -requires synchronized high-speed V/I sampling, DFT computation per cycle, and ATP + MATLAB simulation/processing
[4]	S. Mane et al., (2020)	PF transducer (CT+PT+Arduino UNO)	Electromagnetic relay	0.7277 to 0.9803	3-phase, 415 V, 50 Hz mains; RL load	Low-cost components: Arduino UNO, relays, contactors
[5]	A. Roy et al. (2026)	PT + CT + Zero-Crossing Detector (ZCD), Arduino	Relay-controlled	(0.64-0.715) to (0.94–0.97)	60–200 W	Moderate-to-higher Raspberry Pi Pico W (more expensive than Arduino), PT, CT, ZCD circuits, relay modules, LCD
[6]	V.S. Patil et al. (2024)	CT + PT + ZCD Arduino Uno (ATmega328)	TRIAC-based switching	0.6 to near unity (simulation, three-phase induction motor load)	3 HP, 415 V, 50 Hz three-phase induction motor	Moderate (Arduino ATmega328), CT, PT, ZCD circuits, TRIACs (more expensive than mechanical relays but no arcing risk)
[7]	L. Katche et al. (2021)	AC Voltage and Current Sensor	MOSFET-Relay	0.5 to 0.99	1384 W	Lower-capacitor, relay, sensors
[8]	M.N. Zaidi et al. (2018)	CT, PT, ZCD	Relay	0.85 to 0.90	750 kW	Lower- PIC microcontroller, LM385 op amp, ZCD
[9]	C. M. Nkinyam et al. (2026)	PZEM-004T	Relay Module	0.64 to 0.99	1105 W	Low-cost implementation with estimated payback period of 1,357 operating hours
Proposed system	This work	Sensor-based detection of connected load combination (binary relay states)	Mechanical relay switching of pre-sized capacitor banks per load combination	0.5 to 0.97 (target)	Lab-scale (60–250 W)	Lower- low-cost microcontroller (Arduino), mechanical relays, fixed capacitor banks; no DFT or high-speed sampling required

An important consideration is to avoid increasing the reactive power by adding excessive capacitance, which results in overvoltage and potential damage to the power system [10]. The required capacitance depends on the initial PF, target PF, real power, supply voltage and frequency. At a certain supply voltage, incorporating a calculated capacitance across the load might reduce the supply current. Increasing the capacitance above the calculated value results in an increase of the supply current and reactive power and turns the circuit capacitive. This results in a power loss. A PF over 0.95 is seen in the mining sector, and the industries typically exhibit a power factor ranging from 0.65 to 0.80 [11]. Nahid et al. enhanced the bus voltage profile of the northern Bangladesh transmission network by a capacitor

placement technique utilizing the mixed integer linear programming (MILP) method. Capacitor installation can improve the bus voltage profile [12]. The aim of this paper is to calculate the appropriate value of capacitors for a load, which will result in an improvement of the power factor. In this study, the methodology section covers the mathematical model of capacitor calculation, Proteus simulation, and experimental design for a basic power system. The Results and Discussion section covers the capacitor bank connection to the load, the percentage of reactive power compensated by the proposed APFI system, and a comparison of the simulation and experimental switching results.

II. Methodology

Fig. 2 shows a block diagram of the proposed APFI system using a microcontroller. The microcontroller receives inductive load data of a power system via sensors and controls the connection between the capacitor bank and the power system with mechanical relays.

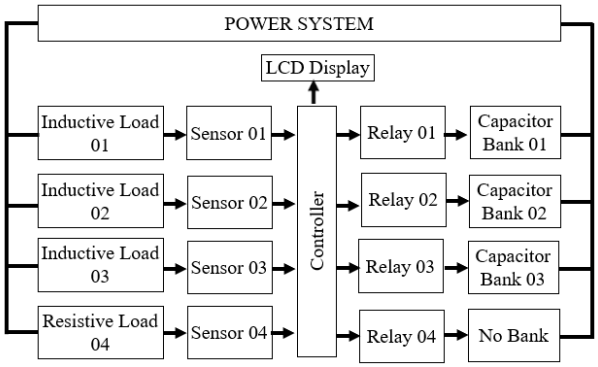


Fig. 2. Block diagram of an APFI system

The programmed microcontroller connects or disconnects the suitable capacitor bank across the load and increases the PF. The proposed system has three inductive loads: choke coil 1, choke coil 2, and an induction motor, denoted as L1, L2, and L3, respectively. A filament bulb is included as the resistive load, L4. The system supply voltage denoted by 'v' is 220 V, and the frequency denoted by f is 50 Hz. Table II presents the real power denoted by P_R and power factor denoted by PF_1 of the connected loads of the proposed APFI system.

TABLE II
LOADS WITH POWER RATINGS

	Choke Coil 1	**Choke Coil 2**	**Induction Motor**	**Filament Bulb**
Symbol	L1	L2	L3	L4
Rated power (W)	160	160	250	60
PF_1 (—)	0.5	0.5	0.6	0.99

The P_R and PF_1 of L1 and L2 are the same. The 'PG 08 Power Guard' measuring instrument is used to measure the P_R and PF_1 of the loads. The proposed APFI system contains three capacitor banks: C1, C2 and C3. The C1 and C2 banks consist of two capacitors (each 2 µF) in parallel. The C3 bank consists of three capacitors (each 2.5 µF) in parallel. The manual switches are used to switch each load on or off. The four AC relays are used to sense the connected or disconnected loads of the APFI system.

A. Mathematical Model of Required Capacitance and Power

Fig. 3 shows the PF improvement diagram for the system's inductive loads: L1, L2 and L3. θ_1 is the phase angle, Q_{a1} is the apparent power and Q_{r1} is the reactive power of the load without the APFI system. θ_2 is the phase angle, Q_{a2} is the apparent power and Q_{r2} is the reactive power after correction. Q_c is the compensated reactive power, equal to $Q_{r1} - Q_{r2}$. The three inductive loads of the power system have a low power factor. A PF of at least 0.9 is generally desirable [13]; a target PF of 0.97, which exceeds this minimum, is used in this work.

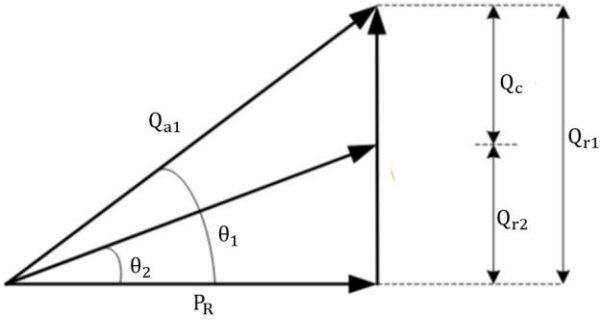


Fig. 3. Power factor improvement diagram

The following equations are used to calculate the required capacitance to be added to the individual inductive load to increase the system power factor. The phase angles θ_1 and θ_2 are obtained from (1) and (2), respectively.

$$PF_1 = \cos\theta_1 \quad (1)$$

$$PF_2 = \cos\theta_2 \quad (2)$$

The real current component denoted by I_R and reactive current component denoted by I_{r1} of the load without APFI are calculated by equations (3) and (4). I_{a1} is the apparent current component of the load without APFI.

$$I_R = I_{a1}\cos\theta_1 \quad (3)$$

$$I_{r1} = I_{a1}\sin\theta_1 \quad (4)$$

In the APFI system, the desired apparent current I_{a2} and desired reactive current I_{r2} are calculated according to equations (5) and (6).

$$I_{a2} = I_{a1}\frac{\cos\theta_1}{\cos\theta_2} \quad (5)$$

$$I_{r2} = I_{a2}\sin\theta_2 \quad (6)$$

The current through the capacitor I_c is calculated by equation (7). The required capacitance, in farads, is calculated by (8).

$$I_c = I_{a1} \sin\theta_1 - I_{a2} \sin\theta_2 \quad (7)$$

$$C = I_c/(2\pi fv) \quad (8)$$

The Q_{a1} is calculated by equation (9).

$$Q_{a1} = P_R/\cos\theta_1 \quad (9)$$

The Q_{a2} is calculated by equation (10).

$$Q_{a2} = P_R/\cos\theta_2 \quad (10)$$

The Q_{r1} is calculated by equation (11).

$$Q_{r1} = Q_{a1} \sin\theta_1 \quad (11)$$

The compensated reactive power Q_c is calculated by equation (12). The percentage of reactive-power compensation, η_c is calculated by equation (13).

$$Q_c = P_R(\tan\theta_1 - \tan\theta_2) \quad (12)$$

$$\eta_c = (Q_c * 100)/Q_{r1} \quad (13)$$

Table III shows the inductive load parameter values calculated by equations (1) to (8). The required capacitance values calculated for L1, L2, and L3 to improve the power factor to 0.97 are C1 = 4 µF, C2 = 4 µF, and C3 = 7.8 µF, respectively. The capacitance values in Table III are expressed in µF (the value of C in (8), in farads, multiplied by 10^6). The real power drawn by each load, PR = Ia1 V cosθ1, is 40.7 W for L1 and L2 and 109.6 W for L3, whereas their rated powers in Table II are 160 W and 250 W; L4 is taken at its rated 60 W.

TABLE III
REQUIRED CAPACITANCE CALCULATION

Symbol	L1	L2	L3
I_{a1} (A)	0.37	0.37	0.83
PF_1 (—)	0.5	0.5	0.6
PF_2 (—)	0.97	0.97	0.97
I_R (A)	0.19	0.19	0.50
I_{r1} (A)	0.32	0.32	0.66
I_{a2} (A)	0.19	0.19	0.51
I_{r2} (A)	0.05	0.05	0.12
I_c (A)	0.27	0.27	0.54
C (µF)	4.00	4.00	7.80

B. Proteus Simulation and Experimental Setup

Fig. 4 shows a code excerpt for capacitor-bank switching while all inductive loads L1, L2 and L3 are on. All the capacitor banks, C1, C2, and C3, are connected to the system. Fig. 5 shows the schematic diagram of the proposed APFI system used in the Proteus simulation. A control method has been established for Arduino to connect the capacitors to the power system. Based on the connected load combination, the microcontroller transmits signals to the relay unit to adjust the reactive power, either by connecting or disconnecting the capacitor bank to improve the power factor. Sensors are used to check the connected load. The microcontroller analyses data from the sensors and executes tasks according to a predetermined control algorithm [14]. The LCD shows the real-time data: power factor and connected loads. Fig. 6 shows the flowchart of the capacitor connecting method of the APFI system. While the APFI system is on, it checks the connected load to the system. There are 15 load combinations to be connected to the system. For a certain load combination, a certain capacitor bank is connected to the system according to the required capacitance. When a load-state condition is satisfied, the corresponding capacitor banks are connected to the system. The connected capacitor bank, connected load, and power factor are shown on the LCD, and the decision cycle ends. If the condition is not satisfied, all the capacitor banks are disconnected from the system, and the system returns to the initial state. The capacitor bank relays used in simulation are in the normally closed position. The displayed active power (W), reactive power (var) and apparent power (VA) are programmed test values used to verify the display and switching logic.

```
if (LS1 == HIGH && LS2 == HIGH && LS3 == HIGH && LS4 == LOW )
   {
     digitalWrite (C1,LOW);
     digitalWrite (C2,LOW);
     digitalWrite (C3,LOW);
                              lcd.setCursor(0,0);     //(C, R)
                              lcd.print("L1=ON  .54>.94 ");
                              lcd.setCursor(0,1);
                              lcd.print("L2=ON  W=570   C1=ON");
                              lcd.setCursor(0,2);
                              lcd.print("L3=ON  VAR=143 C2=ON");
                              lcd.setCursor(0,3);
                              lcd.print("L4=OFF VA =588 C3=ON");
```

Fig. 4. Code of capacitor connection and LCD display

Fig. 7 shows the experimental setup of the APFI system. The manual switchboard consists of four manual switches (S1-S4) and is used to switch the individual loads on or off to test different load combinations. The LCD display shows the connected loads, the connected capacitor banks, and the displayed power factor with the desired power factor. There are four AC-operated relays (R1-R4) to sense the connected load to the system and three DC-operated relays (R5-R7) to connect the capacitor bank to the system. The S1, S2, S3, and S4 switches connect L1, L2, L3, and L4 loads to the system, respectively. The R1, R2, R3, and R4 relays detect the L1, L2, L3, and L4 loads, respectively. The R5, R6 and R7 relays connect C1, C2, and C3 capacitor banks to the system, respectively. The Arduino board controls the relay module and displays system information on the LCD. The red indicator lights indicate relay activation.

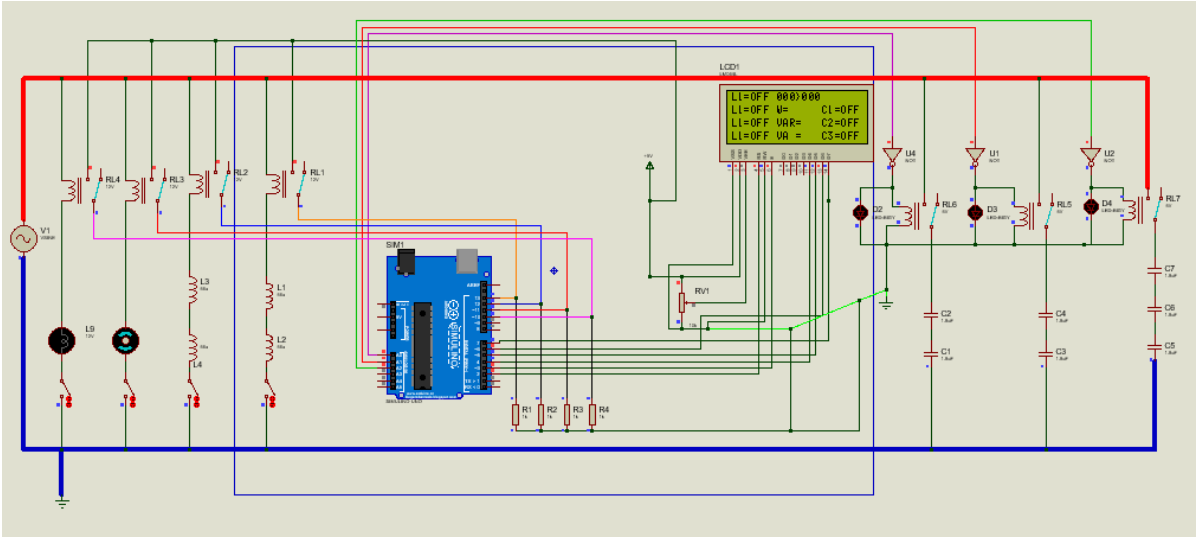


Fig. 5. Schematic diagram of APFI system in Proteus

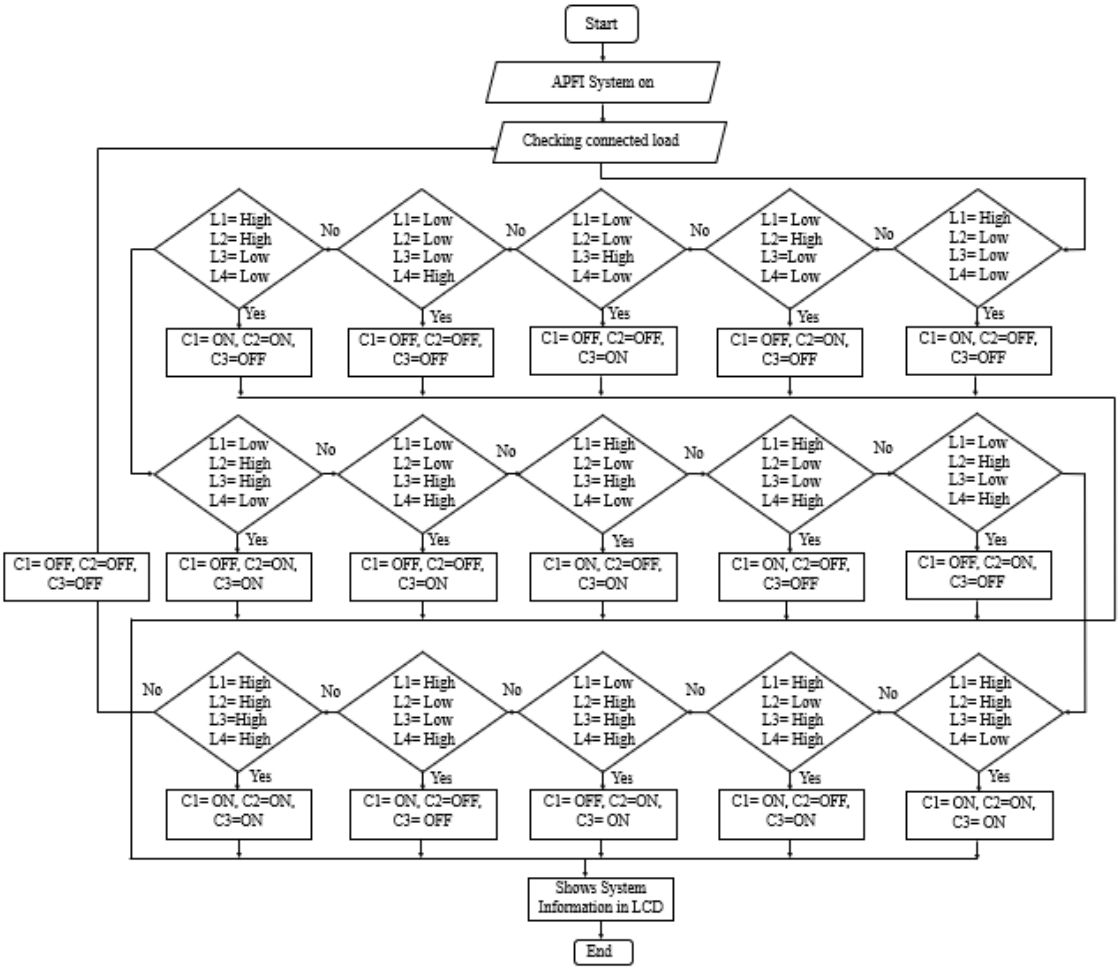


Fig. 6. Flowchart of the capacitor connecting method

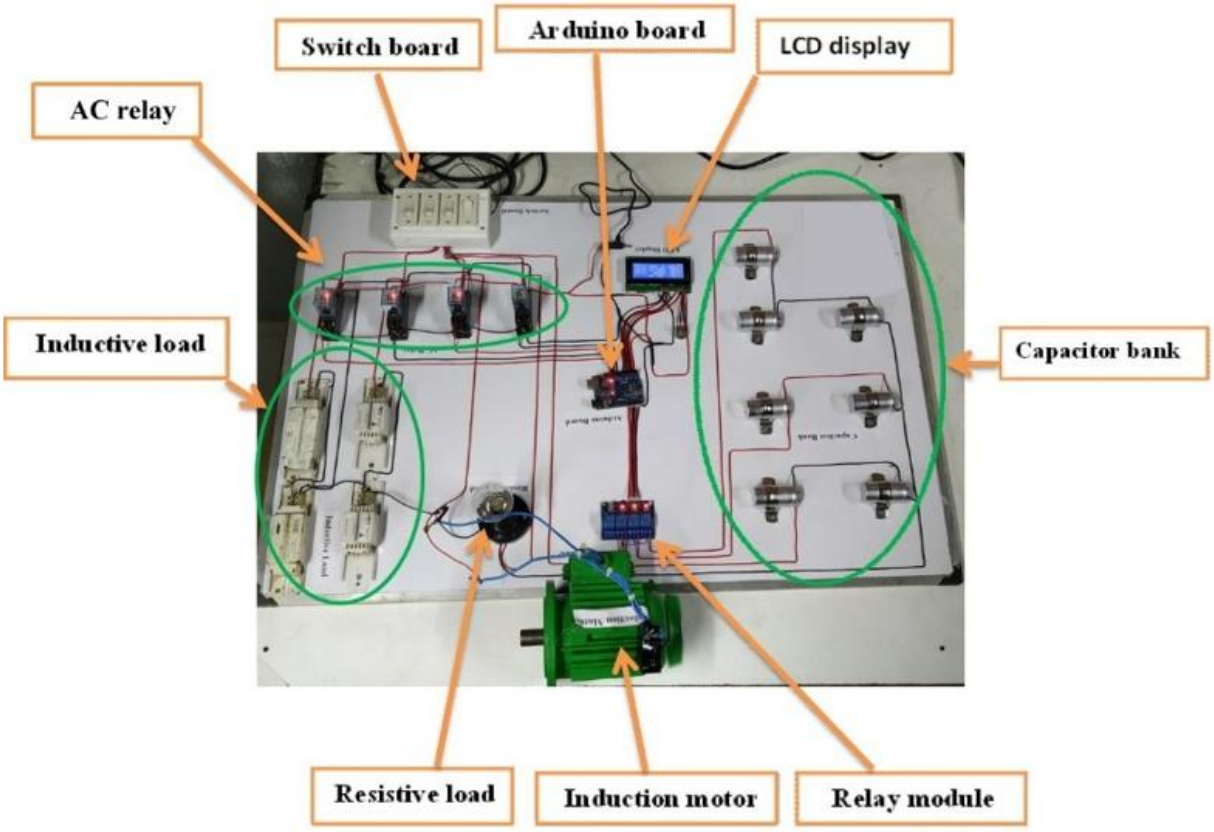


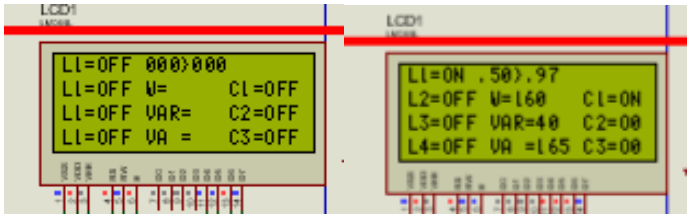
Fig. 7. Hardware implementation of APFI system

III. Results and Discussion

Table IV lists the 15 nonzero load combinations and their calculated parameters. The calculation shows that approximately 73% of the reactive power can be compensated by adding the C3 capacitor bank when L3 and L4 are active, and approximately 79% when all four loads are connected. The calculation shows that, for every load combination that requires correction, Q_{a2} is less than the Q_{a1}. In Fig. 8(a), the Proteus simulation results show that no parameter values are displayed on the LCD when all loads are off. The W, var, VA and PF values displayed in Figs. 8–10 are programmed test values based on the rated powers in Table II, so they differ from Table IV, which uses the real powers calculated from the measured currents in Table III. In Fig. 8(b), the power factor can be improved from 0.50 to 0.97 with L1 on while the remaining loads are switched off. In that condition, capacitor C1 is connected as programmed. In Fig. 9(a), the power factor can be increased from 0.60 to 0.97 while only L3 is operating with all other loads off. In that condition, the capacitor bank C3 is connected to improve the power factor. In Fig. 9(b), the power factor can be improved from 0.55 to 0.97 with L2 and L3 operational, while the rest of the loads are inactive. In that state, the capacitor banks C2 and C3 are connected to improve the power factor. In Fig. 10(a), the power factor can be improved from 0.55 to 0.97 while L1 and L3 are on and L2 and L4 are off. In that scenario, the capacitor banks C1 and C3 are connected. In Fig. 10(b), the power factor can be improved from 0.58 to 0.97 while all loads are switched on by connecting the capacitor banks C1, C2, and C3 to the system.

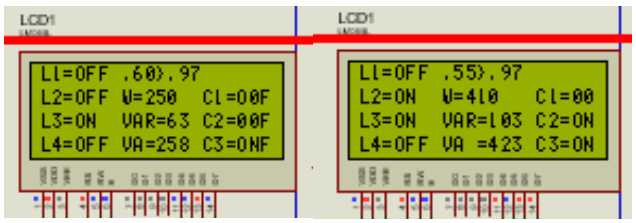
TABLE IV
LOAD COMBINATIONS AND PARAMETER VALUES WITH CONNECTED CAPACITOR BANKS

Load Combinations	P_R (W)	PF_1 (—)	Q_{a1} (VA)	Q_{r1} (var)	PF_2 (—)	Q_c (var)	Q_{a2} (VA)	η_c (%)	Capacitor Bank
L1	41	0.50	81	70	0.97	60	42	86	C1
L2	41	0.50	81	70	0.97	60	42	86	C2
L3	110	0.60	183	146	0.97	119	113	81	C3
L4	60	0.99	61	9	-	-	-	-	-
L1+L2	81	0.50	163	141	0.97	121	84	86	C1+C2
L2+L3	150	0.57	264	217	0.97	179	155	83	C2+C3
L3+L4	170	0.74	229	155	0.97	112	175	73	C3
L1+L3	150	0.57	264	217	0.97	179	155	83	C1+C3
L1+L4	101	0.79	128	79	0.97	54	104	68	C1
L2+L4	101	0.79	128	79	0.97	54	104	68	C2
L1+L2+L3	191	0.55	345	287	0.97	239	197	83	C1+C2+C3
L1+L3+L4	210	0.68	308	225	0.97	172	217	77	C1+C3
L2+L3+L4	210	0.68	308	225	0.97	172	217	77	C2+C3
L1+L2+L4	141	0.69	206	150	0.97	114	146	76	C1+C2
L1+L2+L3+L4	251	0.65	388	296	0.97	233	259	79	C1+C2+C3



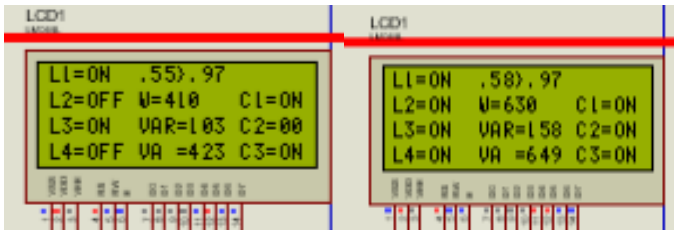
(a) (b)

Fig. 8. (a) L1, L2, L3 and L4 are switched off. (b) L1 is on, and L2, L3 and L4 are switched off. The W, var and VA values shown on the LCD are programmed test values.



(a) (b)

Fig. 9. (a) L3 is switched on, and L1, L2 and L4 are switched off. (b) L2 and L3 are switched on, and L1 and L4 are switched off. The W, var and VA values shown on the LCD are programmed test values.



(a) (b)

Fig. 10. (a) L1 and L3 are switched on, and L2 and L4 are switched off. (b) L1, L2, L3 and L4 are switched on. The W, var and VA values shown on the LCD are programmed test values.

Table V summarizes the experimental relay-switching states of the APFI system. Binary values 0 and 1 denote the off and on states, respectively. For an individual load, when switch S1 is on, load L1 is connected to the system. The Arduino microcontroller detects the connected load L1 by sensing the R1 relay and connects the capacitor bank C1 to the system by activating the R5 relay.

TABLE V
EXPERIMENTAL CAPACITOR-BANK RELAY-SWITCHING STATES

				APFI System						
S1	**S2**	**S3**	**S4**	**R1**	**R2**	**R3**	**R4**	**R5**	**R6**	**R7**
1	0	0	0	1	0	0	0	1	0	0
0	1	0	0	0	1	0	0	0	1	0
0	0	1	0	0	0	1	0	0	0	1
0	0	0	1	0	0	0	1	0	0	0
1	1	1	1	1	1	1	1	1	1	1

When switch S4 is on, load L4 is connected to the system. Load L4 has a near-unity PF, so the capacitor-switching relays R5–R7 remain off. When all switches S1, S2, S3, and S4 are turned on, all the loads, L1, L2, L3, and L4, are connected to the system. The sensing relays R1, R2, R3, and R4 are activated, and all the capacitor banks are connected to the system automatically using the Arduino microcontroller to activate relays R5, R6 and R7.

IV. Conclusion

The APFI system can improve the overall PF of the connected loads. The proposed APFI system connects the capacitor banks automatically, based on the connected load combination, instead of manually.

A. Limitations

Response time, long-term reliability and practical deployment have not been evaluated. The system does not include controlled switching (for example, zero-crossing detection), so capacitor switching may produce inrush current, contact arcing and accelerated wear.

B. Future Work

Response time, long-term reliability and practical deployment will be evaluated in future work. Zero-crossing detection and other inrush-limiting measures, such as series inrush-limiting inductors or solid-state switching, will be investigated to reduce switching stress.

Appendix

NOMENCLATURE

Symbol	Parameter Definition	Unit
PF_1	Load power factor	—
PF_2	Desired load power factor	—
I_R	Load real current	A
I_{a1}	Load apparent current	A
I_{r1}	Load reactive current	A
I_{a2}	Desired apparent current	A
I_{r2}	Desired reactive current	A
I_c	Capacitor current	A
C	Required capacitance	μF
v	Voltage	V
f	Frequency	Hz
P_R	Real power	W
Q_{a1}	Apparent power	VA
Q_{r1}	Reactive power	var
Q_{r2}	Desired reactive power	var
Q_c	Compensated reactive power	var
η_c	Reactive − power compensation	%

Conflict of Interest

The authors declare no conflict of interest.

Author Contributions

Mohammad Iftekher Uddin: supervision, methodology and simulation. Robin Barua: introduction, results and discussion, efficiency calculation and manuscript writing.

References

[1] M. Oommen and J. L. Kohler, "Power factor and power factor control alternatives for mines," in *Conf. Rec. 1988 IEEE Ind. Appl. Soc. Annu. Meeting*, Pittsburgh, PA, USA, 1988, vol. 2, pp. 1209–1215, doi: 10.1109/IAS.1988.25213.

[2] M. Madhiarasan, "Implementation of IoT-based energy monitoring and automatic power factor correction system," *Thermal Sci. Eng.*, vol. 6, no. 1, Apr. 2023, doi: 10.24294/tse.v6i1.1996.

[3] R. A. Mahmoud and A. Emam, "Coherence-based automatic power factor correction (APFC) algorithm for power grids," *J. Eng.*, vol. 2022, no. 5, pp. 512–527, 2022, doi: 10.1049/tje2.12133.

[4] S. Mane, R. Sapat, P. Kor, J. Shelar, R. D. Kulkarni, and J. Mundkar, "Microcontroller based automatic power factor correction system for power quality improvement," in *Proc. Int. Conf. Emerg. Technol. (INCET)*, Belgaum, India, 2020, pp. 1–6, doi: 10.1109/INCET49848.2020.9154008.

[5] A. Roy, G. Anilkumar, M. Najil K, S. C. P, N. Skaria, and E. Paul, "IoT-based automatic power factor correction with real-time carbon footprint estimation," *Int. J. Res. Appl. Sci. Eng. Technol. (IJRASET)*, vol. 14, no. 3, pp. 592–601, Mar. 2026, doi: 10.22214/ijraset.2026.77462.

[6] V. S. Patil, A. Potpose, M. Sakhare, and K. Varpe, "Design and development of TRIAC based automatic power factor correction system," *Int. J. All Res. Educ. Sci. Methods (IJARESM)*, vol. 12, no. 3, pp. 2759–2763, Mar. 2024.

[7] L. Katche Musong, P. Tsafack, and E. Tanyi, "Proposed automatic load-side power factor correction system algorithm and its economic benefits in battery based renewable energy systems," *Int. J. Adv. Sci. Res. Eng.*, vol. 7, no. 6, pp. 14–22, Jun. 2021, doi: 10.31695/IJASRE.2021.34080.

[8] M. N. Zaidi and A. Ali, "Power factor improvement using automatic power factor compensation (APFC) device for medical

industries in Malaysia," *MATEC Web Conf.*, vol. 150, Art. no. 01004, 2018, doi: 10.1051/matecconf/201815001004.

[9] C. M. Nkinyam, T. T. B. Clausel, C. Anyanwu, et al., "Development of a novel IoT-based monitoring and automatic power factor correction system for dynamic load," *J. Elect. Syst. Inf. Technol.*, vol. 13, Art. no. 65, 2026, doi: 10.1186/s43067-026-00371-9.

[10] L. Diaconescu, "Reactive power compensation solutions in the metallurgical industry installations," *Sci. Bull. Elect. Eng. Fac.*, vol. 25, no. 1, pp. 74–81, Jun. 2025, doi: 10.2478/sbeef-2025-0012.

[11] P. M. Shilavant, N. P. Bhonsle, R. S. J, and B. S. C, "Power factor correction for industrial loads," *Int. J. Eng. Res. Technol. (IJERT)*, vol. 10, no. 11, ICEI 2022, 2022.

[12] Nahid-Al-Masood, A. Jawad, K. T. Ahmed, S. R. Islam, and M. A. Islam, "Optimal capacitor placement in northern region of Bangladesh transmission network for voltage profile improvement," *Energy Rep.*, vol. 9, pp. 1896–1909, Dec. 2023.

[13] M. Y. Naqash and Z. Rashid, "PI controller based automatic power factor correction (APFC) using capacitor bank," *Elect. Control Commun. Eng.*, vol. 19, no. 1, pp. 40–48, 2023, doi: 10.2478/ecce-2023-0006.

[14] S. A. Qureshi and N. Aslam, "Efficient power factor improvement technique and energy conservation of power system," in *Proc. 1995 Int. Conf. Energy Manage. Power Del. (EMPD '95)*, Singapore, 1995, vol. 2, pp. 749–752, doi: 10.1109/EMPD.1995.500824.